Pharmaceutical Sciences, 2020, 26(3), 296-305
doi:10.34172/PS.2020.31
https://ps.tbzmed.ac.ir/

Research Article

Improvement of Bioavailability and Dissolution of Tanshinone IIA by Encapsulating it with Hydroxypropyl-β-Cyclodextrin

Jie Yu[1], Ni Wu[1], Xiaohui Zheng[1], Maosheng Zheng[2*]

[1]*School of Life Sciences, Northwest University, Xi'an, 710069, China.*
[2]*School of Chem. Eng., Northwest University, Xi'an, 710069, China.*

Article Info

Article History:
Received: 12 February 2020
Accepted: 14 April 2020
ePublished: 20 September 2020

Keywords:
-Bioavailability
-Drug delivery
-Encapsulation composite
-HP-β-CD
-Tanshinone IIA

Abstract

Background: Tanshinone IIA(TA) could be used for the treatment of some diseases. However, the clinical application of TA was hindered by its poor water - solubility and low oral bioavailability, etc. The aim of this study was to improve its oral bioavailability and dissolution by encapsulating TA with hydroxypropyl–beta–cyclodextrin (HP-β-CD).

Methods: The encapsulation composite of HP-β-CD/TA was prepared through solution method with optimization of response surface test design by taking encapsulation efficiency and drug loading as the goals; the in-vitro dissolution and in-vivo metabolism of the composite in rats were evaluated.

Results: The optimal concentration of HP-β-CD in water was 0.4 g/mL; the optimal ratio of TA to HP-β-CD was 1:7 in weight for the encapsulating process at 50°C with stirring for 2h; the encapsulation efficiency and drug loading were 84.06% and 7.38%, respectively; the cumulative release of TA from HP–β -CD TA composite in vitro dissolution reached to 72% within 90 min, which was 3.78 times of that of the original TA substance; the area under the curves of $AUC_{(0-t)}$ and $AUC_{(0-\infty)}$ of the HP–β –CD -TA inclusion composite were 3.71 and 3.42 times of the original TA substance under $p<0.01$, respectively. The apparent distribution volume V_Z/F and the clearance rate VL_Z/F of HP–β –CD -TA inclusion composite decreased by 7.71 and 3.48 times as compared with the original TA substance, respectively.

Conclusion: The improvements of bioavailability and dissolution by encapsulating TA with HP-β-CD were effective.

Introduction

Tanshinone IIA (TA) is one of the main fat - soluble bioactive ingredient extracted and purified from the root of *Salvia miltiorrhiza Bunge* (Danshen),[1] which has been widely used for the treatment of cardiovascular disorders,[2-9] inflammation[10,11] and cancer.[12-14] Figure 1 showed the chemical structure of TA. However, the clinical application of TA has been hindered by its poor water-solubility (2.8 ng mL^{-1}), short half-life (1-2 h), first passes metabolism, and low oral bioavailability.[15-18]

Recently, numerous new drug delivery systems have been employed to deal with these problems, such as solid dispersion,[15-17] polymer nanoparticle,[18-20] solid liposome nanoparticle,[21] micro-emulsions [22-24] and TA sulfonate,[25] inclusion composite,[26,27] etc. The composition of the products from these methods excluding inclusion composite is complex, which might posse unidentified hazard.

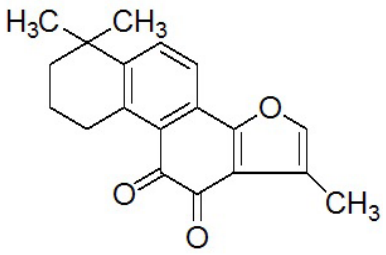

Figure 1. Chemical structure of Tanshinone IIA.

Wang et al reported the preparation of inclusion composite containing TA by co-evaporating with hydroxypropyl – beta - cyclodextrin (HP-β-CD) named as TA/ HP-β-CD at the molar ratio of 1:1.[26,27] The TA / HP-β-CD had significant dissolution rate due to the complexation with HP-β-CD. The absorption behavior of TA and the complexation through the intestinal tissues in vitro were studied without any investigation of in vivo in rats.[26,27] It indicated that inclusion composite with HP-β-CD encapsulation was one of the promising approaches for improving the bioavailability of TA. HP-β-CD comprised of 6 to 8 α-D-glucopyranosides linked by α-1,4-linkages, as a result the highly water-soluble derivatives of HP-β-CD is a useful content that could be used to encapsulate

*Corresponding Author: Maosheng Zheng, E-mail: mszheng2@yahoo.com

numerous hydrophobic compounds into its cavity to improve their aqueous solubility, chemical stability and bioavailability.[28-35] Some research data confirmed its nephrotoxicity based on its administration way. As the first approved CD derivative by FDA, HP-β-CD has wide applications in food, pharmaceuticals and agriculture etc.[36] In view point of pharmacology, the pharmacokinetics of plasma metabolism differences of drug such as TA in vivo in rats was more effective to reflect its actual behavior.

The aim of this study was try to conduct the encapsulation for TA with HP-β-CD through the most commonly used solution method so as to increase the bioavailability of TA, and the dissolution of the composite in vitro and metabolism in vivo in rats are studied ; the response surface test method with taking encapsulation efficiency and drug loading percentage as goals was used to perform the optimization of the encapsulation process of the HP-β-CD-TA inclusion composite.

Materials and Methods

TA (Purity >97%) was purchased from Xi'an Huayang Biological Technology Co. Ltd. (Shaanxi, China); the reference substance of TA (batch number: 110766-201721) was from China National Institute for the Control of Pharmaceutical and Biological Products; HP-β-CD was purchased from Xi'an Deli Biochemical Co., Ltd.; Diazepam Injection (2ml: 10mg) was purchased from Shanghai Xudong Haipu Pharmaceutical Co., Ltd.; Methanol (chromatographically pure) was purchased from Fisher Scientific, USA; Formic acid (analytical grade) was purchased from Tianjin Tianli Chemical Reagent Co., Ltd.; Anhydrous ethanol (analytical grade) was purchased from Tianjin Fuyu Fine Chemical Co., Ltd.; Heparin sodium injection was purchased from Shanghai First Biochemical Pharmaceuticals.

SPF male Sprague-Dawley rats, 230±10 g, were provided by Experimental Animal Center School of Medicine of Xi'an Jiaotong University (license number: SCXK2018-001, Shaanxi, China), and were feed for a week in animal room of the laboratory for adaptability before the official test.

Preparation of HP-β-CD-TA inclusion composite

Solution method has been the most commonly used technique to prepare inclusion composite,[37] which was employed to make the HP-β-CD-TA inclusion composite in this section. The procedure for preparing HP-β-CD-TA inclusion composite was as follows: weigh about 5g of HP – β - CD and dissolve it in 15mL water under normal temperature; weigh 1g of TA powder and dissolve it in 20mL ethanol, then slowly add this solution into the HP-β-CD unsaturated liquid, and stir it with magnetic stirring for some hours at certain temperature. The magnetic stirring was continued to certain time so that the encapsulation of drug molecule was sufficient, and then the unencapsulated drug molecule was removed by washing with petroleum ether three times, the organic solvent was removed by rotary evaporation at 50 °C to obtain an aqueous solution of the clathrate. The clathrate was freeze - dried further to get a clathrate powder. The freeze-drying of the vials was conducted by lyophilization for 24 h with 40 mbar vacuum in a freeze-dryer, secondary drying at 25°C for 8 h. The freeze-dryer is product of SCIENTZ-12N, Ningbo xinzhi biotechnology co. LTD, Ningbo, China.

Analytical methodology

The concentration of TA in the testing medium was quantified by high performance liquid phase chromatographic system (HPLC) of Dalian Elite C5100 Series. The testing condition was: ZORBAX Eclipse XDB-C18 (4.6×250mm, 5um) column, 2‰ formic acid water and methanol (10:90 v/v) as mobile phase at flow rate of 1.0 ml/min, and UV detection at 280 nm. The linearity range of the method was investigated for the concentration from 0.25μg/mL to 50 μg/mL (R^2=0.9997). The relative standard deviation (RSD) of intraday and interday precision for TA was below 3%. The average blank recovery rates of TA in the testing medium at three concentrations (low, medium and high) were 98.13%, 97.60%, and 99.58%, respectively.

The concentration of TA in the plasma content in rats was quantified by HPLC of Dalian Elite C5100 Series as well, which was under condition of ZORBAX Eclipse XDB-C18 (4.6×250mm, 5um) column, HPLC chromatographic gradient elution conditions for 2‰ formic acid water and methanol gradient elution were shown in Table 1, which were with the procedure of mobile phase at flow rate of 1.0 ml/min and UV detection at 280 nm. The standard curve of TA in rat plasma was provided to the Editorial Office of Pharmaceutical Sciences. The fitting result of the standard curve showed that the curve is highly linear within 0.19-25μ/mL. The results were, $y = 140.73x + 4.30$, $R^2 = 0.9993$.

Table 1. Conditions for HPLC gradient elution test.

Time (min)	0	10	11	22	23	33
0.2% Formic acid water: Methanol	30:70	30:70	10:90	10:90	30:70	30:70

Determination of encapsulation efficiency and drug loading

The encapsulation efficiency and drug loading of the encapsulation composite were assessed by using Eq. (1) and Eq. (2).

Optimization of preparation process of HP-β-CD-TA inclusion composite

Optimal design

The preparation process of HP-β-CD-TA inclusion composite was optimized by Design-Expert 8.0.6 software based on the results of single factor experiment for inclusion composite preparation in the preliminary experiment. The concentration of the drug in the preparation was controlled at 1 mg/mL, and the rotation rate of the magnetic stir was 1000 rpm. The Box-Behken response surface test design method was employed to optimize the preparation process by taking encapsulation efficiency and drug loading of the inclusion composite as the goals. The

$$\text{Encapsulation efficiency \%} = \frac{\text{Total amount of tanshinone IIA - free tanshinone IIA in the supernatant}}{\text{Total amount of tanshinone IIA}} \times 100\% \quad \text{Eq. (1)}$$

$$\text{Drug loading \%} = \frac{\text{Total amount of tanshinone IIA - free tanshinone IIA in the supernatant}}{\text{Total amount of tanshinone IIA + amount of carrier material}} \times 100\% \quad \text{Eq. (2)}$$

concentration of HP-β-CD in water, the ratio of drug to carrier material, encapsulating time and temperature were taken as fundamental factors to be optimized to obtain the optimal preparation process of HP – β - CD - TA inclusion composite.

Table 2 showed the fundamental factors and level of Box-Behken test design, and Table 3 listed the design and results for HP-β-CD-TA inclusion composite prepared by Box-Behken test design. In the design, X_1, X_2, X_3 and X_4 in Tables 2 and 3 were independent variables with their meanings shown in Table 2.

Table 2. Fundamental factors and level for Box-Behken test design.

Fundamental factor	Level		
	-1	0	1
X_1: HP-β-CD concentration(mg/mL)	0.3	0.4	0.5
X_2: Ratio of drug to carrier material	1:5	1:6	1:7
X_3: Encapsulating time(h)	1	2	3
X_4: Encapsulating temperature (℃)	40	50	60

Verification test for the prediction

Three batches of HP-β-CD-TA inclusion composite were prepared individually according to the optimal preparation process of the response surface test design. The encapsulation efficiency and drug loading of the three batches of HP-β-CD-TA inclusion composite were tested and averaged. Furthermore, the relationships of the average values for both encapsulation efficiency and drug loading of HP-β-CD-TA inclusion composite with respect to their fundamental factors were fitted to get the corresponding fitting equations by response surface test design method. Afterward, the prediction results from the fitted equations were verified by 3 verification tests.

Fourier-transform infrared spectroscopy (FTIR)

Proper amount of original TA, HP-β-CD, physical mixture of HP-β-CD and TA, and the inclusion composite HP-β-CD-TA were taken individually, which were grinded with KBr powder uniformly and compressed into slice sample, respectively. The FTIR analysis was performed for each slice sample with a Nicolet 5700 Fourier Transform Infrared Spectrometer (Thermo Company, USA), the range of infrared spectra test was in 500 – 4000 cm^{-1}.

The vitro dissolution of HP-β-CD-TA composite

The test for vitro dissolution of HP-β-CD-TA composite was according to procedure of the Chinese Pharmacopoeia 2015 (General Rule 0931, Cause 2 of the Part4). 0.5% sodium dodecyl sulfate solution (900 mL) was the dissolution medium, the rotation rate was 50 rpm, and the temperature was 37±0.5°C. Take a sample of 1 mL at 5, 15, 30, 45, 60, 90, 120, 180, 240 min, respectively, and replenish the same amount of dissolution medium immediately, then filter the sample with 0.45μm microporous membrane. Finally, take 10 μL of the filtrate for HPLC detection. The measurement result was substituted into the standard curve to calculate the concentration. The cumulative dissolution rate at each sampling moment was calculated using Eq. (3). Thereafter a dissolution rate curve could be plotted.

Table 3. Detail of Box-Behken test design and result.

No	Level				Encapsulation efficiency (%)	Drug loading (%)
	X_1	X_2	X_3	X_4		
1	0	1	0	1	73.86	6.43
2	1	0	0	-1	75.38	6.51
3	1	1	0	0	78.55	6.62
4	0	0	1	1	68.18	5.97
5	-1	1	-1	0	69.82	5.65
6	0	1	-1	0	73.33	6.84
7	0	0	-1	-1	76.74	6.63
8	0	-1	1	0	65.56	5.74
9	1	0	-1	0	80.43	7.01
10	0	-1	0	-1	79.73	6.62
11	0	1	1	0	74.22	6.83
12	1	0	0	1	70.32	5.08
13	0	0	0	0	84.77	7.41
14	0	0	1	-1	62.55	4.92
15	0	0	0	0	85.83	7.57
16	0	0	-1	1	65.64	5.45
17	0	0	0	0	83.97	7.28
18	1	-1	0	0	80.39	7.01
19	-1	0	1	0	65.98	4.88
20	0	-1	-1	0	78.49	6.67
21	0	0	0	0	84.91	7.55
22	0	1	0	-1	76.05	6.63
23	-1	0	0	-1	72.17	4.58
24	1	0	1	0	66.55	5.82
25	-1	1	0	0	75.57	6.43
26	0	-1	0	1	67.97	5.58
27	-1	-1	0	0	73.78	5.73
28	0	0	0	0	80.85	7.09
29	-1	0	0	1	65.41	4.57

$$Q = \frac{C_n V + V_0 (C_1 + C_2 + ... + C_{n-1})}{1000W} \quad \text{Eq. (3)}$$

in which Q is the cumulative dissolution rate, C_n is the mass concentration measured in the sample ($mg \cdot L^{-1}$), n is the order of sampling, here the maximum of n is 9 according to the above sampling division of test; V_0 is the volume of each sample (mL), and W is the amount of the inclusion composite (mg), V is the volume of the release medium (mL).

Study of pharmacokinetics of TA composite in rats

The pharmacokinetics was studied to realize the differences of the plasma metabolism of TA in the inclusion composite

and the original TA substance suspension solution in rats by intra - gastric administration comparatively.

The procedure of the preparation of TA substance suspension solution was as follows: accurately weigh the appropriate amount of original TA substance and place it into a mortar, add a certain volume of 0.5% sodium carboxymethyl cellulose solution, grind it to disperse uniformly and form a 8mg/mL TA suspension solution.

The procedure of the preparation of HP-β-CD-TA clathrate solution was as follows: the lyophilized powder of the optimally prepared HP-β-CD-TA encapsulation composite was dissolved in a volume of ultrapure water to make HP-β-CD-TA inclusion composite solution with the concentration of TA by 8mg/mL.

Healthy Sprague-Dawley rats were randomly divided into two groups, 6 rats in each group. The rats were fasted with normal drinking water. After 12 hours, blood 0.6mL was taken from the fundus venous plexus as a blank control. Then, the TA substance suspension solution and the HP-β-CD-TA composite solution were administered by intra-gastric administration, respectively. The dosage was 100 mg/kg (calculated from the content of TA), blood was taken from the fundus venous plexus at 0.25h, 0.5h, 0.75h, 1.0h, 1.5h, 2.0h, 2.5h, 3.0h, 4.0h, 5.0h, 6h, 7h, 10.0 h after administration. The Plasma was placed in a centrifuge tube treated with sodium heparin, and centrifuged at 4°C for 10 min at the speed of 10000 revolutions per minutes (RPM). Then, the serum supernatant was accurately transferred to 100 μL, and 20 μL (50 μg/mL) of diazepam standard solution was added as an internal standard. Diazepam was the basic internal standard material, which was stable in rats. Afterward the protein was precipitated 3 times in amount of acetonitrile by vortexing for 3 min, and then centrifuged at 10000 rpm for 10 min. Finally the supernatant was taken out. The residue was precipitated twice according to the above procedure. All the resulting supernatants were combined together in a centrifuge tube, and then dried by blowing nitrogen to get the solid sample. The solid sample in the centrifuge tube was reconstituted with 100μL of methanol to obtain a solution sample. Then the solution sample was vortexed and centrifuged at 12000 rpm for 10 min at 4°C, the supernatant was taken and filtered through a 0.22μm organic filter to get final sample solution. The final sample solution was kept in refrigerator at 4°C. Take the final sample solution (plasma sample) to conduct test and inject into liquid chromatography according to its conditions, the injection volume was 20 μL, the area of TA peak was recorded, and the content of TA in plasma was calculated.

Statistical analysis for test data and presentation

All data were treated by statistical analysis. The pharmacokinetic parameters were evaluated by the non-compartmental method using DAS 3.0.0 software (Shanghai, China). These parameters included the maximum plasma concentration (C_{max}), the time T_{max} till the maximum plasma concentration (C_{max}), the half-life of elimination ($t_{1/2z}$), the apparent distribution volume V_Z/F, the clearance rate VL_Z/F, the mean residence time (MRT), and the areas under the "curve of drug vs time", i.e., $AUC_{(0-t)}$ and $AUC_{(0-\infty)}$. The "curve of drug vs time" was stood for the curve of TA concentration in the plasmas in vivo in normal rat vs time. One-way ANOVA was used to assess statistical significance at the levels of $^*P < 0.05$, $^{**}P < 0.01$ between the different pairs of formulations.

Results and discussion

Chromatogram of TA

Figure 2 a, b and c showed the comparison of TA chromatogram in plasma spiked sample and chromatogram of the plasma samples after intra-gastric administration. The results indicated the test was effective for the detection of the concentration of TA. The linearity range of this method for the concentration of TA was in 0.19-25 μg/mL (R^2= 0.9993). The limit of quantification of TA was 0.08 μg/mL, and the detection limit was 0.05 μg/mL. The RSD of intraday and interday precision and accuracy for TA were below 3% and 4%, respectively; the RSD of extraction recovery was below 7%; the RSDs for short-term room

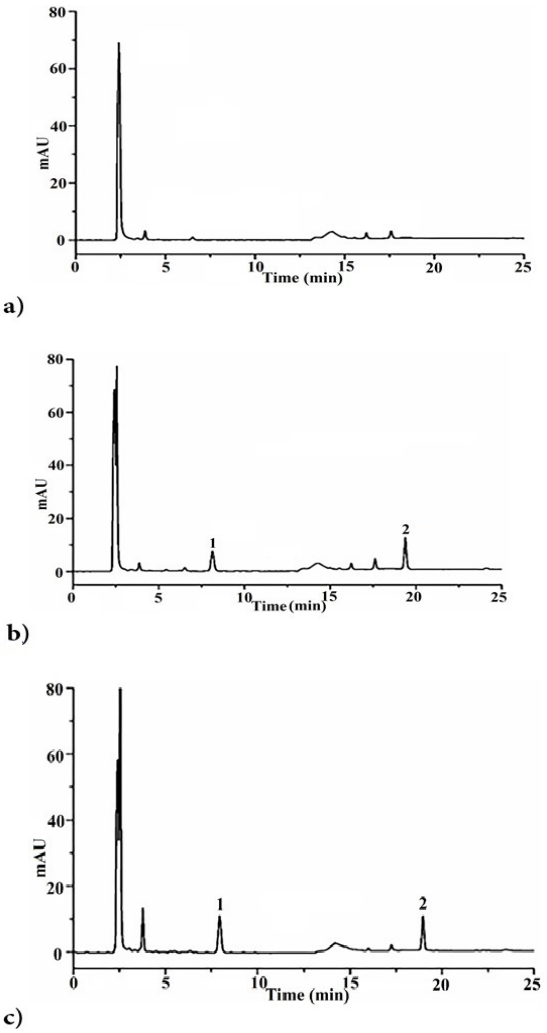

Figure 2. High performance liquid phase chromatogram of Tanshinone IIA
1: Diazepam, 2: Tanshinone IIA
a) Chromatogram of blank plasma sample
b) Chromatogram of blank plasma spiked sample
c) Chromatogram of plasma samples after intragastric administration

temperature stability and long-term stability were below 8% and 10%, respectively; and the RSD of freeze-thaw stability was below 8%.

Optimization using response surface test method

Fitting and analysis with response surface test method

Design-Expert 8.0.6 software was employed to analyze the experimental results listed in the Table 3, and fitted relationships to reflect the variations of encapsulation efficiency and the drug loading with respect to the fundamental factors were obtained. The statistical analysis parameters and variance analysis of the experimental results were listed in Table 4. The statistical parameters for encapsulation efficiency and drug loading were shown in Table 5 and Table 6, respectively.

The binomial equation fitted for the encapsulation efficiency f_e was:

$$f_e = + 84.07+2.41X_1+0.47X_2-3.45X_3 - 2.60X_4 - 0.89X_1X_2 - 2.51X_1X_3 + 0.43X_1X_4 + 3.45X_2X_3 +4.18X_3X_4-5.11X_1^2 - 2.21X_2^2 - 8.46X_3^2 - 7.64X_4^2 \quad \text{Eq. (4)}$$

The binomial equation fitted for drug loading f_c was:

$$f_c = +7.38 + 0.52X_1 + 0.20X_2 - 0.34X_3 -0.23X_4 - 0.27X_1X_2 -0.10X_1X_3 - 0.35X_1X_4 + 0.23X_2X_3 +0.21X_2X_3 + 0.568X_3X_4 - 0.96X_1^2 - 0.057X_2^2 - 0.65X_3^2 - 1.08X_4^2 \quad \text{Eq. (5)}$$

From Table 4, the fitted correlation coefficient R^2 of the inclusion composite and the drug loading were 0.9714 and 0.9505, respectively, and Adj were 0.9428 and 0.9011, respectively, which indicated that the model was promised; the coefficient of variation of the indicators was relatively small, 2.16 and 4.48, respectively. It showed that the credibility and precision of the model were high; the signal – to–noise ratios of the survey indicators were 18.304 and 13.317, respectively, which was greater than 4, it indicated that the response signal of the model was stronger.

From Table 5 and Table 6, it could be seen that both models were promised in statistical significance.

The missing values of the indicators in these model were 69.84 and 3.21, respectively, which were greater than 0.05, it was not significant and without statistical significance, which indicated that the model could give a proper prediction without missing factor.

From Tables 5 and 6, the following results could be seen in the viewpoint of P value: the factors that affected extremely significant the encapsulation efficiency included X_1, X_3, X_4, X_1X_3, X_2X_3, X_2X_4, X_3X_4, X_1^2, X_2^2, X_3^2, and X_4^2; as to drug loading, the factors that affected extremely significant were X_1, X_3, X_4, X_3X_4, X_1^2, X_3^2, and X_4^2; the P values of X_1^2, X_3^2, and X_4^2 were all less than 0.0001; the most significant factors that affected the encapsulation efficiency and drug loading of the inclusion composite were these three factors: X_1 (concentration of HP-β-CD), X_3 (encapsulating time) and X_4 (encapsulating temperature). Above results showed that the models could be used to accurately analyze and predict the experimental results, and the optimization for the preparation process of HP-β-CD-TA inclusion composite could be conducted.

The optimal preparation process of the inclusion composite could be obtained by deriving the maximums of Eqs (4) and (5) with respect to the fundamental factors, X_1, X_2, X_3 and X_4, respectively.

Table 4. Statistical analysis parameters of the experimental results.

	Coefficient of variation (%)	Signal to noise ratio	Correlation coefficient (R^2)	Correction decision coefficient (Adj)
Encapsulation efficiency	2.16	18.304	0.9714	0.9428
Drug loading	4.48	13.317	0.9505	0.9011

Table 5. Results of statistical analysis for encapsulation efficiency in inclusion composite.

Source of variance	Sum of square	Degree of freedom	Mean square	F value	P value
model	1223.87	14	87.42	33.94	<0.0001**
X_1	69.84	1	69.84	27.12	0.0001**
X_2	2.61	1	2.61	1.01	0.3309
X_3	142.90	1	142.90	55.48	<0.0001**
X_4	81.33	1	81.33	31.58	<0.0001**
X_1X_2	3.19	1	3.19	1.24	0.2848
X_1X_3	25.20	1	25.20	9.78	0.0074**
X_1X_4	0.72	1	0.72	0.28	0.6047
X_2X_3	47.75	1	47.75	18.54	0.0007**
X_2X_4	22.90	1	22.90	8.89	0.0099**
X_3X_4	69.97	1	66.97	27.17	0.0001**
X_1^2	169.08	1	169.08	64.64	<0.0001**
X_2^2	31.73	1	31.73	12.32	0.0035**
X_3^2	463.75	1	663.75	180.05	<0.0001**
X_4^2	387.79	1	378.79	147.06	<0.0001**
Residual	36.06	14	2.58	--	--
Missing value	21.39	10	2.14	0.58	0.7773
Pure error	14.67	4	3.67	--	--
Total deviation	1259.93	28	--	--	--

Note: 1) *P<0.05 indicates significance 2) ** P<0.01, indicating that it is extreme significance.

Table 6. Results of statistical analysis for drug loading in the inclusion composite.

Source of variance	Sum of square	Degree of freedom	Mean square	F value	P value
model	21.03	14	1.50	19.22	<0.0001**
X_1	3.21	1	3.21	41.12	<0.0001**
X_2	0.49	1	0.49	6.30	0.0250*
X_3	1.39	1	1.39	17.84	0.0009**
X_4	0.66	1	0.66	8.42	0.0116*
X_1X_2	0.30	1	0.30	3.80	0.0716
X_1X_3	0.044	1	0.044	0.56	0.4650
X_1X_4	0.50	1	0.50	6.45	0.0236*
X_2X_3	0.21	1	0.21	2.71	0.1221
X_2X_4	0.18	1	0.18	2.26	0.1552
X_3X_4	1.24	1	1.24	15.91	0.0013*
X_1^2	6.00	1	6.00	76.82	<0.0010**
X_2^2	0.021	1	0.021	0.27	0.6112
X_3^2	2.72	1	2.72	34.75	<0.0001**
X_4^2	7.53	1	7.53	96.28	<0.0001**
Residual	1.09	14	0.078	--	--
Missing value	0.93	10	0.093	0.92	0.2147
Pure error	0.16	4	0.040	--	--
Total deviation	22.12	28	--	--	--

Note: 1) *P<0.05 indicates significance 2) ** P<0.01, indicating that it is extreme significance.

Table 7. Results of verifying experiment.

Dependent variable	Test value (%)	Averaged test value (%)	Predicted value (%)	Deviation(%)
	80.81			
Encapsulation efficiency	82.67	81.79	84.06	-2.7
	81.88			
	7.35			
Drug loading	7.25	7.30	7.38	-1.1
	7.29			

Note: deviation % = [(average measured value - predicted value)/predicted value]× 100%

The optimized fundamental factors were obtained, i.e., the HP-β-CD concentration in water was 0.4g/mL, the ratio of drug to carrier material was 1:7, and the encapsulating time and temperature were 2h and 50°C, respectively. Substituting these optimized factors into the fitting equations, the predicted encapsulation efficiency was 84.06%, and the predicted drug loading was 7.38%, respectively.

Verification of the predictions by experiments

The experimental results for verifying the predictions were shown in Table 7.

As could be seen from Table 7 that the averaged encapsulation efficiency and drug loading of tests were 81.79% and 7.30%, respectively, of which the deviation from the predicted value was less than 3%, it indicated that the model was reliable, and could be used to conduct prediction accurately.

Infrared characterization

Figure 3 a, b, c and d showed the infrared characteristic absorptions of TA, HP-β-CD, simple mixture of TA and HP-β-CD, and HP-β-CD-TA inclusion composite, respectively.

As could be seen from Figure 3 a), TA had a significant C=O absorption peak at 1670.4 cm^{-1}. The spectra of pure HP-β-CD and HP-β-CD-TA inclusion composite could be seen from Figure 3 b) and Figure 3 d). The peak shape on the upper part had a high degree of similarity, so it could be inferred that the basic skeleton structure of HP-β-CD had not changed during the encapsulation. Niloy et al once studied the host - guest encapsulation of active alkaloid Trigonelline hydrochloride (TgC) and hydroxypropyl – β – cyclodextrin, the comparison of FTIR spectra of both simple physical mixture and inclusion complex was used to confirm the formation of the encapsulated complex of TgC in hydroxypropyl–β–cyclodextrin encapsulation. The disappearance of absorption band between 3084 and 3040 cm^{-1} was attributed to the insertion of the C-H from $-CH_3$ and $C^{sp}{}_2$ - H from aromatic ring into the cavity of the cyclodextrin moiety,[29] thus it confirmed the formation of the encapsulated complex of TgC in hydroxypropyl-β-cyclodextrin encapsulation.[29] Similarly, here the simple physical mixture of HP – β - CD and TA, and the inclusion complex of HP-β-CD-TA were comparatively shown in Figsure 3 c) and d). As could be seen from Figure 3 c), the absorption peaks in the simple physical mixture of TA and HP-β-CD were the simple superposition of the absorption peaks of TA and HP-β-CD. However, in the inclusion complex diagram of Figure 3 d), the sharp characteristic absorption peak of the carbonyl C=O at 1670 cm^{-1} of TA disappeared, which was due to the shielding effect of HP-β-CD encapsulation to TA drug molecule owing to the latter entering into the cavity of after the inclusion reaction, so

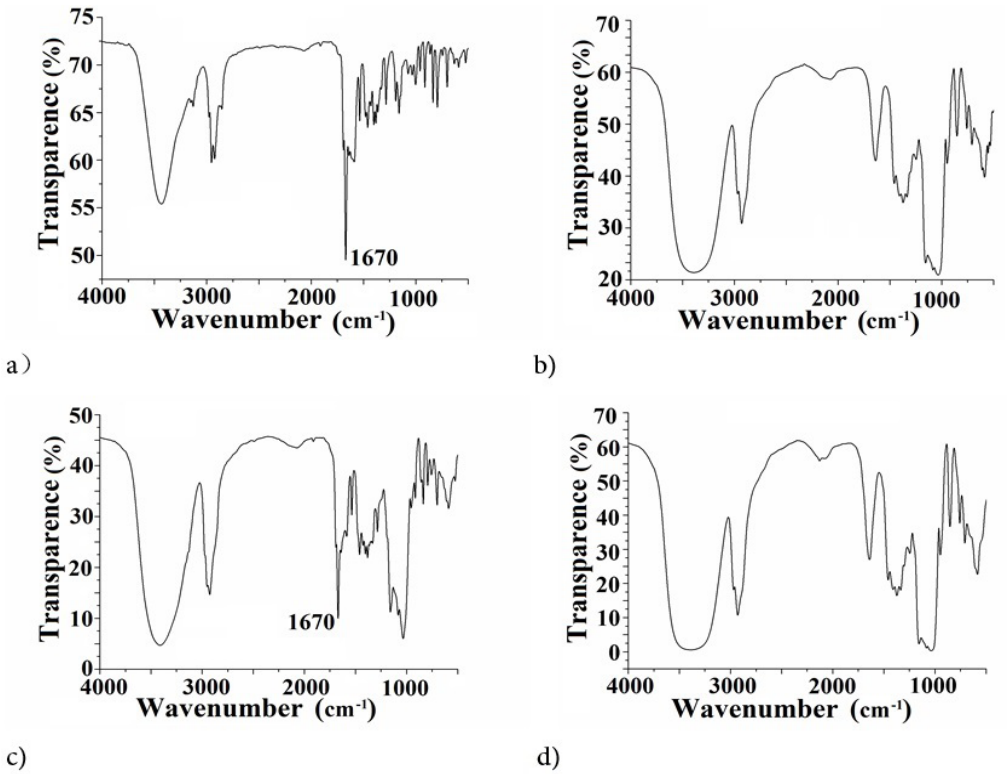

Figure 3. Comparison of infrared characteristic spectra of inclusion composite, mixture and original substances of Tanshinone IIA and hydroxypropyl–β–cyclodextrin
a) Tanshinone IIA, b) hydroxypropyl–β–cyclodextrin, c) simple mixture of hydroxypropyl –β–cyclodextrin and Tanshinone IIA, d) inclusion composite of hydroxypropyl –β–cyclodextrin - Tanshinone

the formation of HP-β-CD-TA inclusion complex was confirmed by the above comparative analysis.[29]

In vitro dissolution test results of HP-β-CD-TA inclusion composite

Figure 4 indicated that the dissolution of TA by HP-β-CD encapsulation was improved greatly, and the cumulative release quantity of TA from the HP-β-CD-TA inclusion composite reached to 72% within 90 min, which is 3.78 times that of the original TA substance. This is due to the dispersing and wetting actions of HP-β-CD to TA by HP-β-CD-TA inclusion composite in water,[26,27,37,38] which enhanced the apparent water - solubility of TA significantly,[26,27,37,38] however the original TA has poor water - solubility (2.8 ng mL^{-1}). So the results in Figure 4 reflected that improvement of in vitro cumulative release of TA by HP-β-CD-TA inclusion composite was significant.

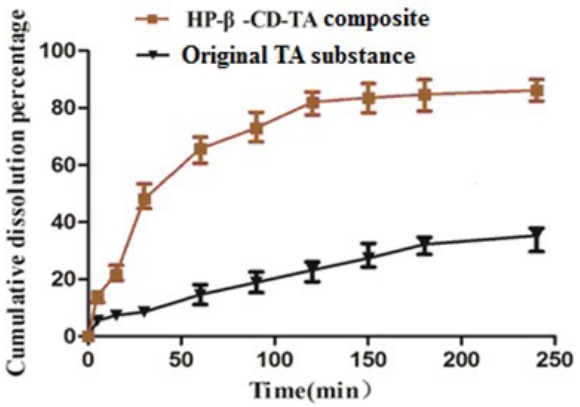

Figure 4. Improvement of in vitro cumulative release of Tanshinone IIA encapsulated by hydroxypropyl – β – cyclodextrin , n = 3.

Pharmacokinetics of TA in the plasmas in normal rats

Figure 5 showed the comparison of curves of TA concentration in the plasmas in vivo in normal rat vs time (drug vs time curve) for the original TA substance and HP-β-CD-TA inclusion composite by intragastric administration.

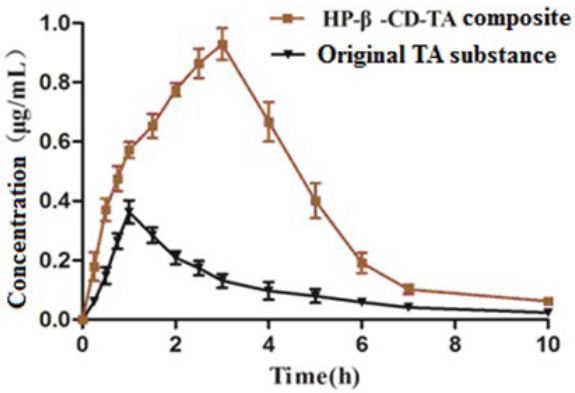

Figure 5. Comparison of Tanshinone IIA concentration vs time in plasma in rats by intragastric administration of Tanshinone IIA encapsulated by hydroxypropyl – β – cyclodextrin and the original Tanshinone IIA substance with dosage of 100 mg/kg (content of Tanshinone IIA), n = 6.

Table 8. Pharmacokinetic parameters for original TA substance group and HP-β-CD-TA inclusion composite in 6 rats by intragastric administration.

Parameter	Unit	Original TA drug substance	HP-β-CD-TA composite
$AUC_{(0-t)}$	mg/ml*h	62.488±9.291	232.211±12.146**
$AUC_{(0-\infty)}$	mg/L*h	69.061±10.686	236.211±9.313**
$MRT_{(0-t)}$	h	184.727±9.27	201.092±5.299
$MRT_{(0-\infty)}$	h	251.911±40.002	212.189±20.69
$t_{1/2z}$	h	186.606±58.949	83.261±59.596
t_{max}	h	60±0	180±0
V_Z/F	L/kg	314738.404±99377.655	40789.895±29408.458
VL_Z/F	L/h/kg	1180.569±172.784	339.051±13.173
C_{max}	mg/L	0.363±0.039	0.929±0.054**

Note: **P < 0.01, indicating extremely significant, n = 6.

It could be seen from Figure 5 that the time Tmax till the concentration peak of TA of the original TA substance group in the drug-time curve was 60 min, however the corresponding time for the inclusion composite group was 180 min; the peak concentration Cmax of the former was 0.363 μg/ml and later was 0.929 μg/ml i.e., the peak concentration C_{max} of inclusion composite group was 2.6 times that of the original TA substance group.

Table 8 showed the pharmacokinetic parameters for original TA substance group and HP–β –CD-TA inclusion composite in 6 rats by intragastric administration.

The experimental results in Table 8 showed that the both $AUC_{(0-t)}$ and $AUC_{(0-\infty)}$ were significantly different in the inclusion composite and the original TA substance under P<0.01, $AUC_{(0-t)}$ and $AUC_{(0-\infty)}$ of HP-β-CD-TA clathrate were 3.71 times and 3.42 times of the original TA substance, respectively. The apparent distribution volume V_Z/F and clearance rate VL_Z/F of the inclusion composite were lower than that of the original TA substance, which was 7.71 times and 3.48 times lower than that of the original TA substance.

It showed that the retention time of the TA in inclusion composite in the body was much longer than that of the original TA substance. Moreover, the T_{max} till TA concentration peak C_{max} of the inclusion composite was much higher than that of the original TA substance in vivo in rats, which was attributed the much larger amount of TA absorption with HP-β-CD-TA inclusion composite in the body.[37,38]

The ratio of bioavailability of TA in HP-β-CD-TA inclusion composite to that of the original TA substance in vivo in rats could be defined as the relative bioavailability of TA in HP-β-CD-TA inclusion composite by Eq. (6):

$$F(\%) = [AUC_{(0-\infty)} \text{ composite } / AUC_{(0-\infty)} \text{ orig.}] \times 100\% \quad \text{Eq. (6)}$$

The relative bioavailability F defined by Eq. (6) could reflect the improvement of bioavailability of TA by HP-β-CD encapsulation comprehensively. The relative bioavailability of TA from HP-β-CD-TA inclusion composite in vivo in tats was 342%.

Conclusion

The optimum preparation process of the inclusion composite was as follows: the concentration of HP-β-CD in water was 0.4g/mL; the ratio of TA to HP-β-CD was 1:7 in weight; the encapsulating time and temperature were 2h and 50°C, respectively.

HP-β-CD inclusion composite greatly improved the in vitro dissolution of TA, the cumulative release quantity of the inclusion composite reached to 72% within 90 min, which was 3.78 times that of the original TA substance.

The relative bioavailability of TA in vivo in tats was increased to 342% in HP-β-CD-TA inclusion composite.

All above results indicated the effectiveness of encapsulating TA with HP-β-CD to improve its dissolution and bioavailability.

Ethical Issues

The study protocol was approved by the Institutional Review Board and ethical committee of Life Sciences School of Northwest University, China. (Approval Number: NWU-AWC-20180301R).

Acknowledgements

The authors would like to greatly acknowledge the Project of Key Research and Development Program of Shaanxi (No. 2019SF-056, No.2017ZDCXL-SF-01-02-01) and the program for Changjiang Scholars Innovative Research in University (No.IRT_15R55) China, for their supports.

Conflict of Interests

The authors claim that there is no conflict of interest.

References

1. Li Z, Xu S, Liu P. *Salvia miltiorrhiza* Burge (Danshen): A golden herbal medicine in cardiovascular therapeutics. Acta Pharmacol Sin. 2018;39:802-24. doi:10.1038/aps.2017.193
2. Zhang X, Wang Q, Wang X, Chen X, Shao M, Zhang Q, et al. Tanshinone IIA protects against heart failure post-myocardial infarction via AMPKs/mTOR-dependent autophagy pathway. Biomed Pharmacother. 2019;112:108599. doi:10.1016/j.biopha.2019.108599
3. Wang N, Chang Y, Chen L, Guo YJ, Zhao YS, Guo QH, et al. Tanshinone IIA protects against chronic intermittent hypoxia-induced myocardial injury via activating the endothelin 1 pathway. Biomed Pharmacother. 2017;95:1013-20. doi:10.1016/j.biopha.2017.08.036
4. Feng J, Chen HW, Pi LJ, Wang J, Zhan DQ. Protective

effect of tanshinone IIA against cardiac hypertrophy in spontaneously hypertensive rats through inhibiting the Cys-C/Wnt signaling pathway. Oncotarget. 2017;8(6):10161-70. doi:10.18632/oncotarget.14328
5. Wei B, Li WW, Ji J, Hu QH, Ji H. The cardioprotective effect of sodium tanshinone IIA sulfonate and the optimizing of therapeutic time window in myocardial ischemia/reperfusion injury in rats. Atherosclerosis. 2014;235(2):318-27. doi:10.1016/j.atherosclerosis.2014.05.924
6. Li X, Du JR, Yu Y, Bai B, Zheng XY. Tanshinone IIA inhibits smooth muscle proliferation and intimal hyperplasia in the rat carotid balloon-injured model through inhibition of MAPK signaling pathway. J Ethnopharmacol. 2010;129(2):273-9. doi:10.1016/j.jep.2010.03.021
7. Liu M, Yang J, Li M. Tanshinone IIA attenuates interleukin-17A-induced systemic sclerosis patient-derived dermal vascular smooth muscle cell activation via inhibition of the extracellular signal-regulated kinase signaling pathway. Clinics (Sao Paulo). 2015 ;70(4):250-6. doi:10.6061/clinics/2015(04)06
8. Chen L, Guo QH, Chang Y, Zhao YS, Li AY, Ji ES. Tanshinone IIA ameliorated endothelial dysfunction in rats with chronic intermittent hypoxia. Cardiovasc Pathol. 2017;31:47-53. doi:10.1016/j.carpath.2017.06.008
9. Li YH, Xu Q, Xu WH, Guo XH, Zhang S, Chen YD. Mechanisms of protection against diabetes-induced impairment of endothelium-dependent vasorelaxation by Tanshinone IIA. Biochimica et Biophysica Acta (BBA). 2015;1850(4):813-23. doi:10.1016/j.bbagen.2015.01.007
10. Liu X, Meng J. Tanshinone IIA ameliorates lipopolysaccharide-induced inflflammatory in bronchial epithelium cell line BEAS-2B by down-regulating miR-27a. Biomed Pharmacother. 2018;104:158-64. doi:10.1016/j.biopha.2018.05.021
11. Wang SB, Guo XF, Weng B, Tang SP, Zhang HJ. Tanshinone IIA attenuates ovalbumin-induced airway inflammation and hyperresponsiveness in a murine model of asthma. Iran J Basic Med Sci. 2019;22(2):160-5. doi:10.22038/ijbms.2018.30598.7375
12. Wu Q, Zheng K, Huang X, Li L, and Mei W. Tanshinone-IIA-Based Analogues of Imidazole Alkaloid Act as Potent Inhibitors to Block Breast Cancer Invasion and Metastasis in vivo. J Med Chem. 2018;61(23):10488-501. doi:10.1021/acs.jmedchem.8b01018
13. Lin J, Ke Y, Lai J, Ho T. Tanshinone IIA enhances the effects of TRAIL by downregulating survivin in human ovarian carcinoma cells. Phytomedicine. 2015;22(10):929-38. doi:10.1016/j.phymed.2015.06.012
14. Xia X and Liu M. [The effect of tanshinone IIA and salvianolic acid B on hepatocellular carcinoma HepG2 cell line and its mechanism]. Zhong Yao Cai. 2014;37(4):652-5. Chinese
15. Luo C, Yang Q, Lin X, Qi C, Li G. Preparation and drug release property of tanshinone IIA loaded chitosan-montmorillonite microspheres. Int J Biol Macromol. 2019;125:721–9. doi:10.1016/j.ijbiomac.2018.12.072
16. Luo CY, Wu W, Lin X, Li Y, Yang K. A novel tanshinone IIA/chitosan solid dispersion: Preparation, characterization and cytotoxicity evaluation spheres. J Drug Deliv Sci Technol. 2019;49:260–7. doi:10.1016/j.jddst.2018.11.024
17. Zhai X, Li C, Lenon GB, Xue CCL, Li W. Preparation and characterisation of solid dispersions of tanshinone IIA, cryptotanshinone and total tanshinones. Asian J Pharm Sci. 2017;12(1):85-97. doi:10.1016/j.ajps.2016.08.004
18. Mao S, Wang L, Chen P, Lan Y, Guo R, Zhang M. Nanoparticle-mediated delivery of Tanshinone IIA reduces adverse cardiac remodeling following myocardial infarctions in a mice model: role of NF-κB pathway. Artif Cells Nanomed Biotechnol. 2018;46(sup3):S707-S716. doi:10.1080/21691401.2018.1508028
19. Li Z, Zhang Y, Zhang K, Wu Z, Feng N. Biotinylated-lipid bilayer coated mesoporous silica nanoparticles for improving the bioavailability and anti-leukaemia activity of Tanshinone IIA. Artif Cells Nanomed Biotechnol. 2018;46(sup1):578-87. doi:10.1080/21691401.2018.1431651
20. Yan HX, Li J, Li ZH, Zhang WL, Liu JP. Tanshinone IIA-loaded pellets developed for angina chronotherapy: deconvolution - based formulation design and optimization, pharmacokinetic and pharmacodynamic evaluation. Eur J Pharm Sci. 2015;76:156–64. doi:10.1016/j.ejps.2015.05.012
21. Chen T, Yang J, Chen L, Qian X, Zheng Q, Fu T, et al. Use of ordered mesoporous silica-loaded phyto-phospholipid complex for BCS IV class plant drug to enhance oral bioavailability: a case report of Tanshinone II_A. RSC Adv. 2016;6:115010-20. doi:10.1039/C6RA22778C
22. Wang W, Chen J, Li M, Jia H, Han X, Zhang J, Zou Y, Tan B, Liang W, Shang Y, Xu Q, A S, Wang W, Mao J, Gao X, Fan G, Liu W. Rebuilding Postinfarcted Cardiac Functions by Injecting TIIA@PDA Nanoparticle-Cross-linked ROS-Sensitive Hydrogels. ACS Appl Mater Interfaces. 2019;11(3):2880-90. doi:10.1021/acsami.8b20158
23. Chu T, Zhang Q, Li H, Ma WC, Zhang N, Jin H, et al. Development of intravenous lipid emulsion of tanshinone IIA and evaluation of its anti-hepatoma activity in vitro. Int J Pharm. 2012;424(1-2):76–88. doi:10.1016/j.ijpharm.2011.12.049
24. Lu X, He L, Chen JN, Li MY, Pan YF. Preparation and in vitro dissolution evaluation of tanshinone IIA for oral self-microemulsion. Chin Trad Herbal Drugs. 2014;45(22):3256-65. Chinese doi:10.7501/j.issn.0253-2670.2014.22.008
25. Zhang K. Analysis of the causes of adverse reactions caused by sodium tanshinone IIA sulfonate injection. Chinese pharmacist. 2011;14(9):1357-8. Chinese
26. Wang L, Jiang X, Xu W, Li C. Complexation of tanshinone IIA with 2-hydroxypropyl-beta-cyclodextrin: effect on aqueous solubility, dissolution rate, and intestinal absorption behavior in rats. Int J Pharm. 2007;341(1-2):58-67. doi:10.1016/j.ijpharm.2007.03.046
27. Ling W, Xuehua J, Chenrui L, et al. Investigation of the improved effects of 2-hydroxypropyl-β-cyclodextrin

on solubility, dissolution rate, and intestinal absorptive profile of tanshinone IIA in rats. Arch Pharm Res. 2007;30:1020. doi:10.1007/BF02993972
28. Marcolino ALP, Macedo LB, Nogueira-Librelotto DR, Fernandes J, Bender CR, Wust KM, e t al. Preparation, characterization and in vitro cytotoxicity study of dronedarone hydrochloride inclusion complexes. Mater Sci Eng C. 2019;100:48-61. doi:10.1016/j.msec.2019.02.097
29. Roy N, Ghosh R, Das K, Roy D, Ghosh T, Roy MN. Study to synthesize and characterize host-guestencapsulation of antidiabetic drug (TgC) and hydroxypropyl - β - cyclodextrin augmenting the antidiabetic applicability in biological system. J Mol Struct. 2019;1179:642-50. doi:10.1016/j.molstruc.2018.11.049
30. Xiao CF, Li K, Huang R, He GJ, Zhang JQ, Zhu L, et al. Investigation of inclusion complex of Epothilone A with cyclodextrins. Carbohydr Polym. 2014;102:297-305. doi:10.1016/j.carbpol.2013.11.049
31. Hsu CM, Tsai FJ and Tsai YH. Inhibitory effect of Angelica sinensis extract in the presence of 2-hydroxypropyl-β-cyclodex. Carbohydr Polym. 2014;114:115-22. doi:10.1016/j.carbpol.2014.07.042
32. Lima PSS, Lucchese AM, Araújo-Filho HG, Menezes PP, Araújo AAS, Quintans-Júnior LJ, et al. Inclusion of terpenes in cyclodextrins: Preparation, characterization and pharmacological approaches. Carbohydr Polym. 2016 Oct 20;151:965-87. doi:10.1016/j.carbpol.2016.06.040
33. Terauchi M, Tamura A, Yamaguchi S, Yui N. Enhanced cellular uptake and osteogenic differentiation efficiency of melatonin by inclusion complexation with 2-hydroxypropyl β-cyclodextrin. *Int J Pharm*. 2018;547(1-2):53-60. doi:10.1016/j.ijpharm.2018.05.063
34. Maniyazagan M, Chakraborty S, Pérez-Sánchez H, Stalin T, Thambusamy S. Encapsulation of triclosan within 2-hydroxypropyl–β–cyclodextrin cavity and its application in the chemisorption of rhodamine B dye. J Mol Liq. 2019;282:235-43. doi:10.1016/j.molliq.2019.02.113
35. Pinho E, Grootveld M, Soares G, Henriques M. Cyclodextrins as encapsulation agents for plant bioactive compounds. Carbohydr Polym. 2014;101:121-35. doi:10.1016/j.carbpol.2013.08.078
36. Brewster ME, Loftsson T. Cyclodextrins as pharmaceutical solubilizers. Adv Drug Deliv Rev. 2007;59(7):645-66. doi:10.1016/j.addr.2007.05.012
37. Frömming KH, Szejtli J. Cyclodextrins in Pharmacy. Springer, Dordrecht; 1994. p83-126. doi:10.1007/978-94-015-8277-3
38. Azzi. J, Jraij A, Auezova L, Fourmentin S, Greige-Gerges H. Novel findings for quercetin encapsulation and preservation with cyclodextrins, liposomes, and drug - in – cyclodextrin – in - liposomes. Food Hydrocoll. 2018;81:328-40. doi:10.1016/j.foodhyd.2018.03.006